Stabilization of a Carbon Support by Surface Oxygen with Respect to Nitrogen Dioxide in the Pd/HOPG Model System

M. Yu. Smirnov[a], *, A. V. Kalinkin[a], and V. I. Bukhtiyarov[a]

[a] Boreskov Institute of Catalysis, Siberian Branch, Russian Academy of Sciences, Novosibirsk, 630090 Russia
*e-mail: smirnov@catalysis.ru

Abstract—In this work, X-ray photoelectron spectroscopy (XPS) was used to study the effect of preliminary oxidative treatment of a carbon support surface on the results of NO_2 interaction with model systems prepared by palladium deposition onto highly oriented pyrolytic graphite (HOPG). It was found that, in Pd/HOPG samples with the atomic ratios $[O]/[C] \leq 0.0035$, the carbon support was oxidized with the destruction of its structure to a depth of 10−15 graphene layers. In this case, the palladium particles remained in a metallic state, and they penetrated into the near-surface layer of the support due to the deep oxidation of adjacent carbon atoms. At the atomic ratio $[O]/[C] \approx 0.01−0.02$, the result of the interaction changed dramatically. In this case, the support remained stable, and the palladium particles were oxidized to form an oxide. This finding explained the high stability of supported palladium catalysts prepared on Sibunit carbon supports in oxidative catalysis reactions.

INTRODUCTION

Palladium catalysts supported on carbon supports are used for selective hydrogenation [1−6], dehydrogenation [7], reductive dehalogenation [8], the Heck reaction [1, 9], and many other processes [10] including electrochemical oxidation in fuel cells [11−14]. Sibunit, a technical mesoporous carbon with a high degree of graphitization, is widely used as a support [15], which has high mechanical strength and resistance to a reaction medium [16−25], in particular, in oxidative catalysis processes [26]. We found that the carbon support in Pd/Sibunit catalysts demonstrated stability in interaction with NO_2 at temperatures ranging from room temperature to 300°C and a pressure of $10^{-6}−10^{-5}$ mbar [27]. At the same time, it was shown in other our works that the support in the Pd/highly oriented pyrolytic graphite (HOPG) system was subjected to intense oxidation, which led to the degradation of 10−15 graphene layers in the structure and the formation of various surface oxygen-containing carbon compounds, at the above pressures of NO_2 already at room temperature [28, 29]. In this case, palladium particles retained a metallic state and penetrated deep into the graphite. It was suggested that Sibunit is stable due to the presence of oxygen atoms on its surface,

Abbreviations and notation: HOPG, highly oriented pyrolytic graphite; XPS, X-ray photoelectron spectroscopy; SEM, scanning electron microscopy; STM, scanning tunneling microscopy; E_b, binding energy; E_{kin}, kinetic energy.

which block the sites of the most probable initiation of carbon support oxidation [27]. In the case of the Pd/HOPG system studied previously [28, 29], oxygen was almost absent from the graphite surface at the moment of deposition of metal particles.

In this work, we used X-ray photoelectron spectroscopy (XPS) to study the interactions of NO_2 with samples prepared by vacuum deposition of palladium metal on HOPG with the varied oxygen content of its surface in order to find out whether oxygen atoms can participate in the stabilization of graphite with respect to oxidizing agents when it is chosen as a carbon support.

EXPERIMENTAL

The XPS spectra were recorded using a SPECS spectrometer (Germany). The conditions of the measurement and processing of the spectra were described in detail elsewhere [28, 29]. Good electrical contact between the samples and the holder was ensured due to the high conductivity of graphite, which excluded charging during the recording of spectra and, as a result, eliminated the need to correct the measured binding energies E_b. Atomic ratios were calculated from the intensities of corresponding photoemission lines taking into account the atomic sensitivity factors taken from a reference book [30].

Palladium was supported onto the surface of graphite by vacuum deposition according to a procedure

Table 1. List of the tested Pd/HOPG samples with indication of palladium particle sizes d_{Pd}, [Pd]/[C] and [O]/[C] atomic ratios, and the conditions of sample preparation and treatment in NO_2

Sample	[Pd]/[C]	[O]/[C]	d_{Pd}, nm	Duration of support bombardment with Ar^+ ions, s	Conditions of modification with oxygen	Conditions of treatment in NO_2, mbar × min
Pd/C	0.0067	0.0004	4[1]	0	No treatment in O_2	10^{-6} × 60
Pd/C-A	0.0047	0.0035	3[1]	10	No treatment in O_2	10^{-5} × 30
Pd/C(O)	0.0165	0.0093	4–6[2]	0	30°C, 20 min	10^{-4} × 30
Pd/C-A(O)	0.0227	0.0233	ND[3]	30	300°C, 20 min	5×10^{-6} × 60

[1] The average particle size of Pd was determined by scanning tunneling microscopy (STM). [2] The particle size of Pd was determined by scanning electron microscopy (SEM). [3] The particle size was not determined.

described previously [28, 29, 31]. A series of samples, which differed in the concentrations of O atoms on the support surface before the stage of metal deposition, was prepared (Table 1). The oxygen content in Table 1 is given as the atomic ratios [O]/[C]. The Pd/C sample was obtained using the initial graphite annealed for several hours in an ultrahigh vacuum at 600°C. Prior to the metal deposition procedure, oxygen on the surface of the initial HOPG occurred in an insignificant amount corresponding to [O]/[C] = 0.0004. The Pd/C-A sample was prepared on a support that had been preliminarily etched with Ar^+ ions without additional oxygen treatment. A small amount of oxygen appeared on the surface in the course of etching, [O]/[C] = 0.0035, due to residual gases present in the preparation chamber and in the argon injection line (Table 1). The Pd/C(O) sample was obtained on graphite exposed to air at atmospheric pressure and room temperature without pretreatment with Ar^+ ions. In the preparation of the Pd/C-A(O) sample, HOPG subjected to ion etching before deposition of the metal was additionally kept in air at 300°C; as a result, a significant oxygen concentration was reached on its surface (Table 1). Henceforth, the Pd/C(O) and Pd/C-A(O) samples are conventionally referred to as oxidized samples.

The amount of deposited palladium in the samples was estimated by the atomic ratio [Pd]/[C] calculated from a ratio between the Pd $3d$ and C $1s$ line intensities taking into account the atomic sensitivity factors (Table 1). The ratio [Pd]/[C] varied in a range from 0.0067 to 0.0227. According to the data of scanning tunneling microscopy (STM) and/or scanning electron microscopy (SEM), the average size of palladium particles in the test samples increased only from 3 to 6 nm with [Pd]/[C] despite a significant scatter in the surface concentrations of palladium; this fact justified a qualitative comparison of the results of the action of NO_2 on the carbon support in the Pd/HOPG samples.

The samples with deposited Pd were treated with nitrogen dioxide obtained by the thermal decomposition of lead nitrate using a source whose design and principle of operation were described elsewhere [31].

The interaction with NO_2 was carried out at the sample temperature close to room temperature.

RESULTS AND DISCUSSION

Figure 1 shows the C $1s$ spectra of palladium samples on HOPG (Fig. 1a) before and (Fig. 1b) after treatment in NO_2. Graphite was subjected to various pretreatment procedures before deposition of the metal. Table 1 summarizes the conditions under which graphite was processed and the resulting palladium samples subsequently reacted with NO_2. All spectra shown in Fig. 1a exhibit a line with the binding energy E_b = 284.4 eV and a characteristic asymmetric shape, which corresponds to sp^2 hybrid carbon in graphite [32−36]. A peak of plasmon losses at 290.6 eV can be seen on the tail of the line [33−35, 37, 38]. After interaction with NO_2, the spectrum of the sample prepared by Pd deposition onto the initial HOPG (Pd/C) underwent significant changes, which manifested themselves in the disappearance of a line with E_b = 284.4 eV due to sp^2 hybrid carbon and the appearance of new lines with higher binding energies (Fig. 1b, spectrum 1). Additional C $1s$ lines recorded in spectrum 1 after interaction with NO_2 were assigned to sp^3 hybrid carbon atoms having no bonds with oxygen atoms (285.0 eV) [34, 39−42], carbon atoms with single C−O bonds in ether and phenolic groups (285.9 eV), [26, 40−47] and double C=O bonds in carbonyl groups (287.3 eV) [26, 43, 46, 48−51].

Similar changes occurred in the sample of palladium deposited on graphite preliminarily subjected to ion etching (Pd/C-A) (Fig. 1b, spectrum 2); however, judging by the presence of a line with E_b = 284.4 eV in the spectrum, the degree of conversion of sp^2 carbon in this case was lower than that in the Pd/C sample. As follows from the pairwise comparison of corresponding spectra 3 and 4 in Figs. 1a and 1b, the C $1s$ region did not undergo any significant changes in the oxidized samples, the preparation procedure of which included the stage of treatment of a carbon support with atmospheric air.
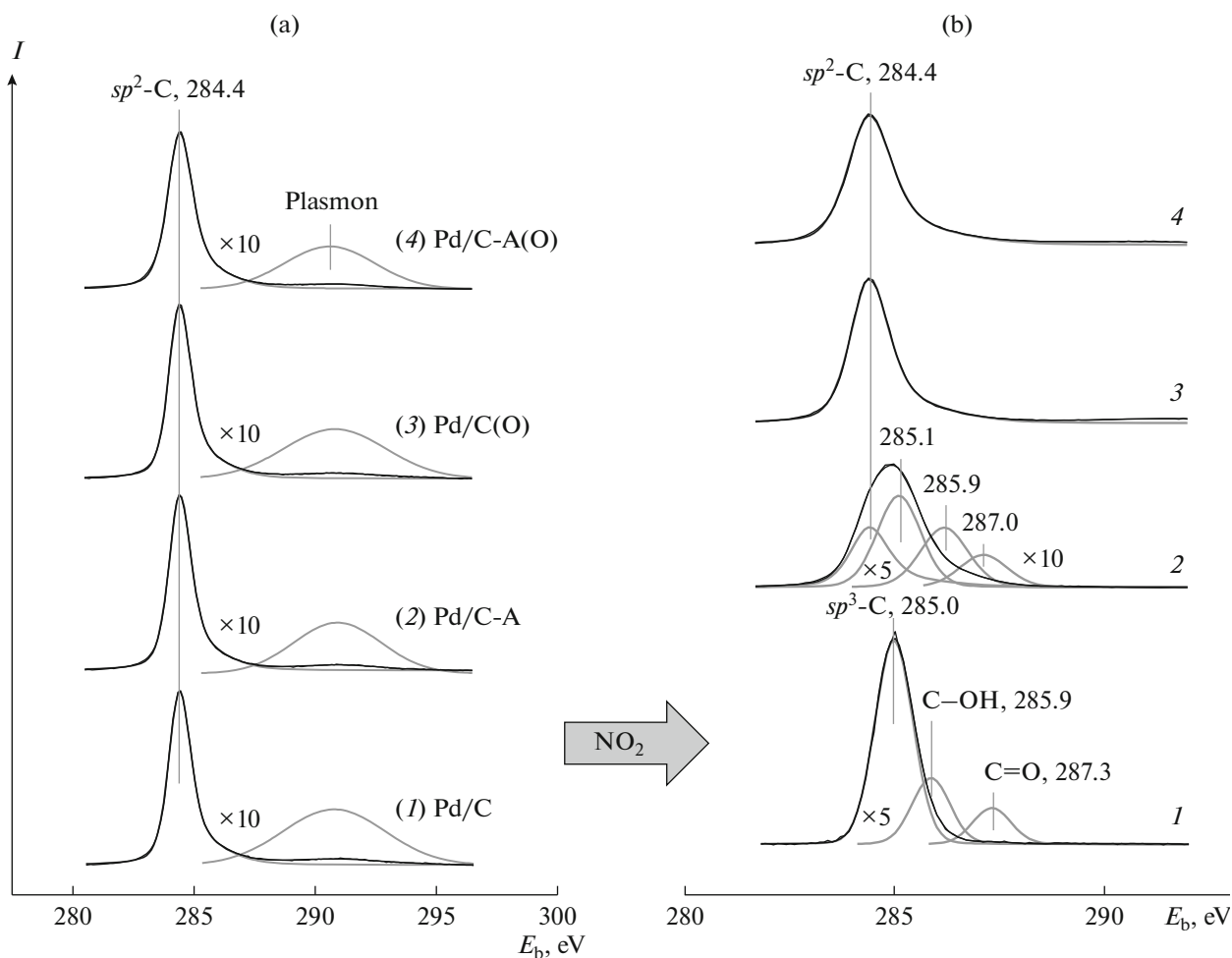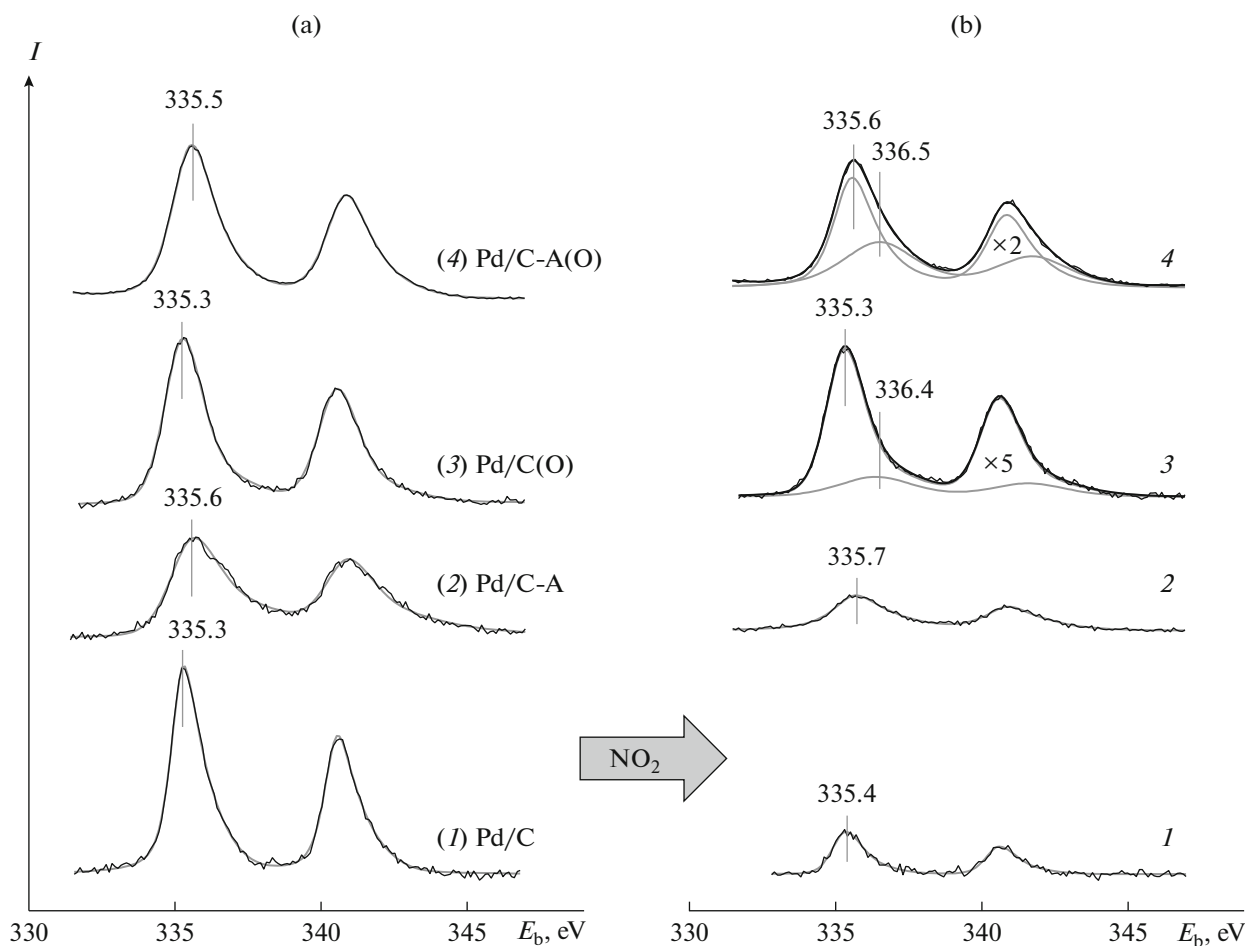
Fig. 1. C 1s spectra of the samples of Pd deposited on HOPG with various preliminary surface preparations (a) before and (b) after interaction with NO_2 under the conditions specified in Table 1.

Figure 2 shows the Pd 3d spectra of samples recorded (Fig. 2a) before and (Fig. 2b) after treatment in NO_2. For all samples in the initial state (Fig. 2a), the spectrum was a doublet with the binding energy E_b(Pd 3$d_{5/2}$) = 335.3–335.6 eV and an asymmetric shape of spin-orbital components, which is characteristic of palladium in a metallic state. The binding energy in the samples was somewhat higher than that of bulk metal (335.2 eV), and it corresponds to E_b(Pd 3$d_{5/2}$) of palladium nanoparticles deposited onto carbon supports [24, 26, 38, 52–54]. After the interaction of the Pd/C and Pd/C-A samples with NO_2, the positions and shapes of the Pd 3d lines did not undergo significant changes, and this fact indicates that the palladium particles retained their original metallic state (Fig. 2b). At the same time, the intensity of the Pd 3d lines decreased. In the oxidized Pd/C(O) and Pd/C-A(O) samples, the decrease in the integral intensity of the Pd 3d line after interaction with NO_2 was not so noticeable, but the appearance of a second doublet with the binding energy E_b(Pd 3$d_{5/2}$) = 336.4–336.5 eV,

which should be attributed to palladium oxide [55–65], was observed. In the Pd/C-A(O) sample, the fraction of PdO was ~23% on a total deposited palladium. In the interaction with NO_2, palladium in the oxidized samples demonstrated behavior similar to that in the previously studied Pd/Sibunit system, in which the formation of palladium oxide was observed after treatment in NO_2 at a pressure of 10^{-6}–10^{-5} mbar and temperatures $T \geq 200°C$ [27].

The Pd M_{45} VV Auger spectra of samples before interaction with NO_2 were characterized by two lines with kinetic energies of 326.4–327.3 and 331.0–331.9 eV (Fig. 3a), which should be attributed to small particles of metallic palladium [62]. We can conclude that a significant portion of palladium in all samples retained a metallic state after the interaction with NO_2 because the positions of lines remained almost the same (Fig. 3b). The bulk palladium oxide PdO exhibited one broad line with a complex shape in this region with the average kinetic energy $E_{kin} \approx 325$ eV [61]. The most significant changes after treatment in NO_2 occurred with
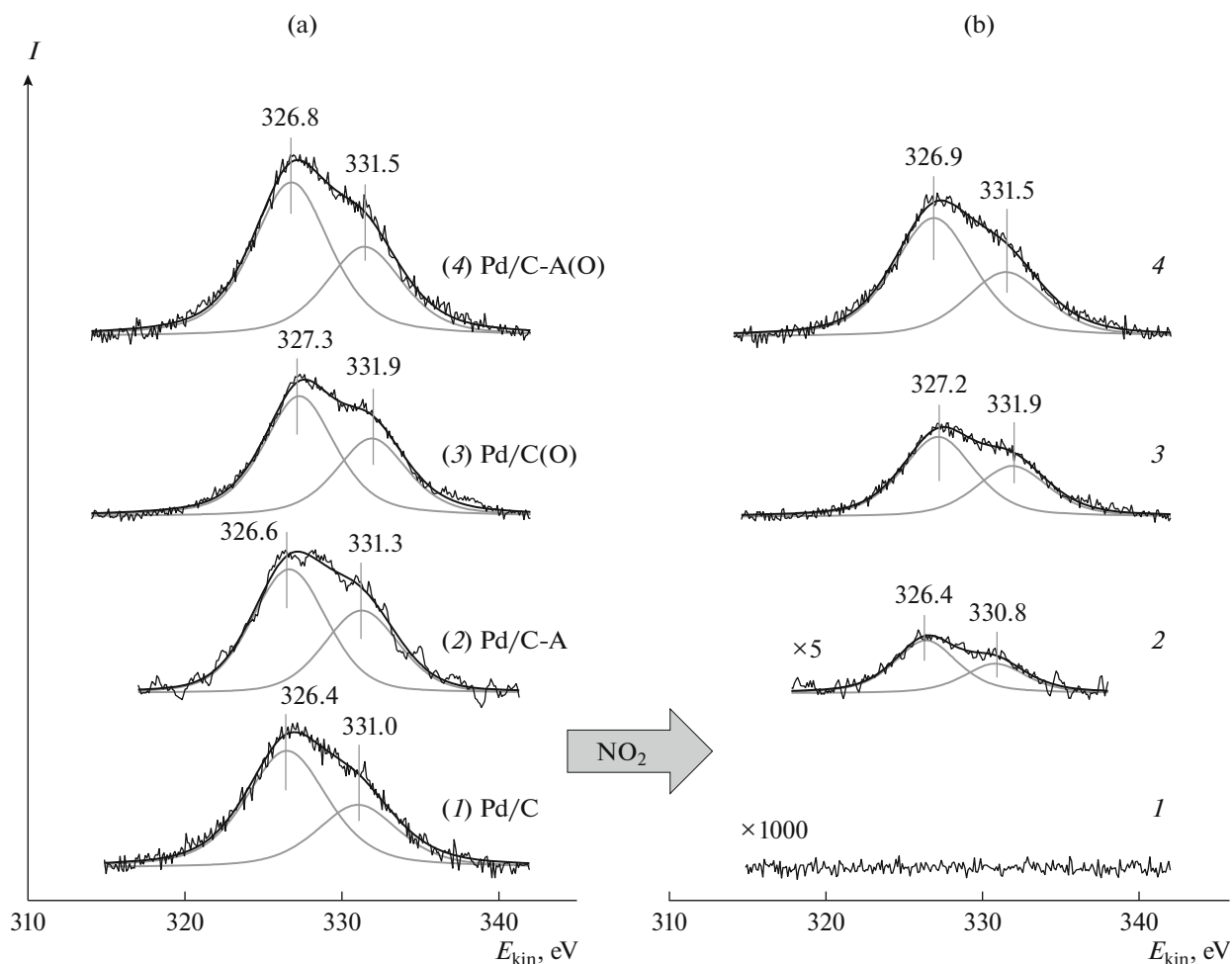
Fig. 2. Pd 3*d* spectra of the samples of Pd deposited on HOPG with various preliminary surface preparations (a) before and (b) after interaction with NO_2 under the conditions specified in Table 1.

the intensities of the Pd $M_{45}VV$ lines. The lines weakened many times in the Pd/C-A sample, and they became unobservable in the spectrum of the Pd/C sample. On the contrary, the Auger line intensities decreased insignificantly in the oxidized samples (Fig. 3b, spectra *3* and *4*).

The intensity of palladium lines can decrease as a result of the interaction of Pd/HOPG samples with NO_2 due to the occurrence of two different processes: an increase in the particle size of the deposited metal (sintering) and the introduction of particles into the near-surface region of the support (encapsulation). In both cases, with the retention of the total amount of deposited palladium, the intensity decreased due to signal screening for a portion of Pd atoms by other atoms of this metal in the former case and for all atoms in Pd particles by the support material in the latter case. It should be noted that the Pd $M_{45}VV$ Auger line is more sensitive to screening than the Pd 3*d* photoemission line due to a significantly lower kinetic energy of Auger electrons, which causes a smaller escape depth for them. This should lead to a more sig-

nificant attenuation of the Auger signal compared to the signal of the photoemission line, which can be seen in Figs. 2 and 3 for the spectra of the Pd/C and Pd/C-A samples. If the interaction with NO_2 leads only to the sintering of palladium particles without their encapsulation by the support, the intensity ratio I_{MVV}/I_{3d} of the two lines should decrease with the particle size and asymptotically approximate to the value inherent in the bulk metal [28, 29]. However, the drop in the intensity ratio for the Pd/C and Pd/C-A samples after treatment in NO_2 was so large that it cannot be explained solely by particle sintering. Thus, it should be recognized that palladium metal particles were inserted into graphite during the interaction of these samples with NO_2 [28, 29]. For the Pd/C(O) and Pd/C-A(O) samples, the intensity ratio did not decrease so significantly; therefore, it can be considered that the incorporation of palladium particles into the support was very insignificant, if any.

The study of oxygen lines for samples containing palladium is difficult to perform because of the mutual overlap of the O 1*s* and Pd $3p_{3/2}$ lines. However, it was

Fig. 3. Pd $M_{45} VV$ Auger spectra of the samples of Pd deposited on HOPG with various preliminary surface preparations (a) before and (b) after interaction with NO_2 under the conditions specified in Table 1.

possible to analyze this spectral region for the Pd/C-A and Pd/C-A(O) (Figs. 4a and 4b, respectively) samples and compare the behaviors of these samples with respect to their interaction with NO_2. The spectrum of the HOPG-A support (Fig. 4a, spectrum *1*) contained one low-intensity O 1*s* line with a binding energy of 532.5 eV. The spectrum of this support pretreated in oxygen, HOPG-A(O), was characterized by two lines with E_b(O 1*s*) = 531.2 and 533.0 eV and a much higher intensity (Fig. 4b, spectrum *1*). These lines can be assigned to oxygen-containing carbon compounds with ether C−O−C or phenolic C−OH [26, 41, 43−46] and carbonyl C=O [26, 43, 46, 48−51] groups, respectively. In the analysis of the spectra of samples with deposited palladium in this region, these O 1*s* lines were taken into account under the assumption that their binding energies, widths at half maximum, and $I_{O1s}(531.2)/I_{O1s}(533)$ intensity ratios are the same as those in the spectrum of the HOPG-A(O) support without palladium. Under these assumptions, the binding energies of the Pd $3p_{3/2}$ line in the Pd/C-A and

Pd/C-A(O) samples prior to interaction with NO_2 are 532.8 and 532.5 eV, respectively (Fig. 4a, spectrum *2* and Fig. 4b, spectrum *2*), which are 0.3−0.5 eV higher than the value measured for bulk palladium [55], probably, due to the small particle size. The metallic state of the particles was confirmed by the appearance of a plasmon near the Pd $3p_{3/2}$ line, which was ~6 eV higher from the main line on the binding energy scale [55, 56]. The intensity of oxygen lines in the oxidized sample Pd/C-A(O) noticeably decreased, and the O 1*s* lines in the Pd/C-A sample became indistinguishable against the background of the Pd $3p_{3/2}$ line, apparently, as a result of screening by palladium particles of the support with oxygen atoms bound to its surface. After the treatment of Pd/C-A in NO_2, the intensity of the O 1*s* line in the region under consideration sharply increased and the line acquired a value of E_b = 533.5 eV, while the Pd $3p_{3/2}$ line became barely distinguishable against the O 1*s* line (Fig. 4a, spectrum *3*). In the Pd/C-A(O) sample, the intensity of the O 1*s* lines did not increase so significantly; however, at the same
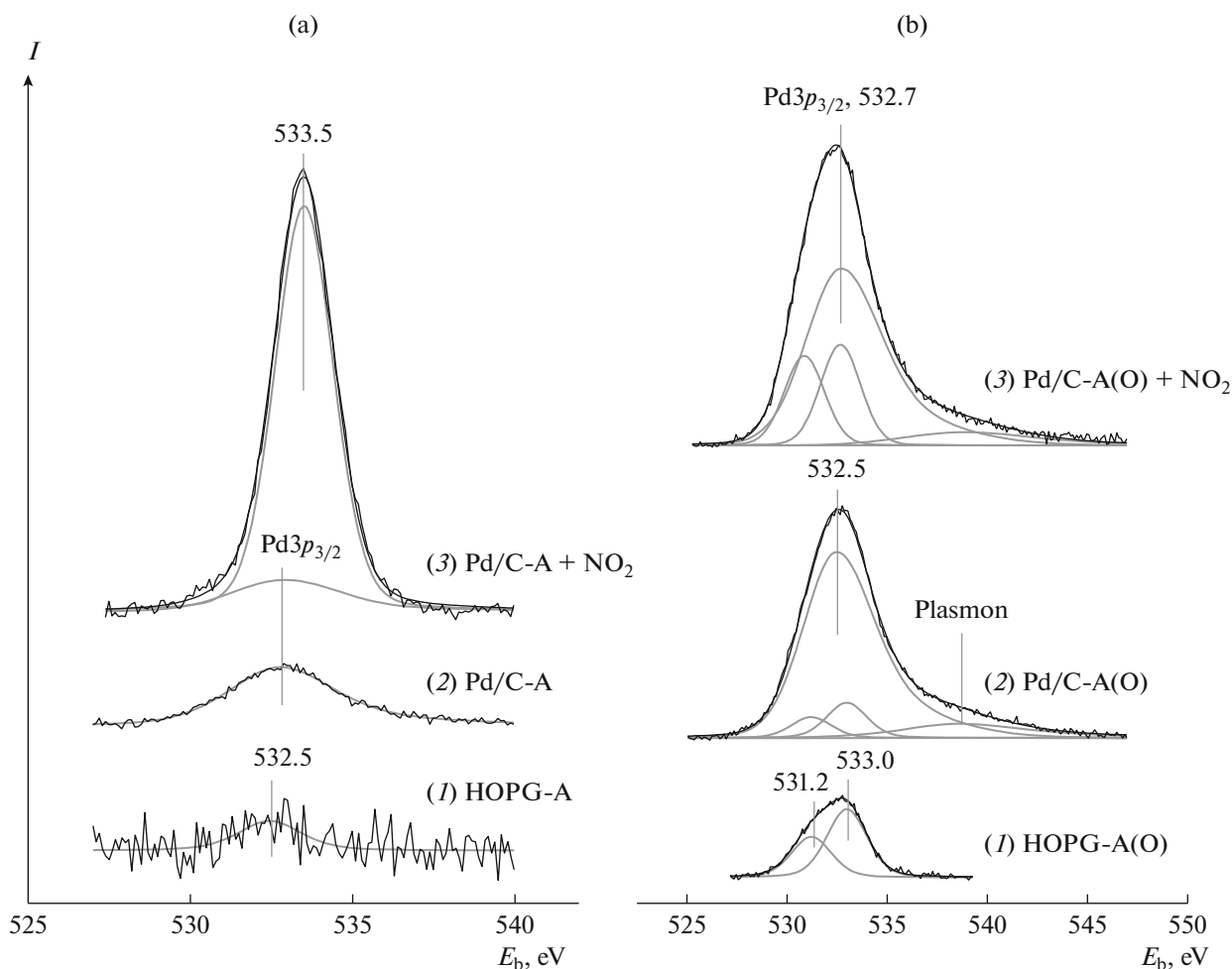
Fig. 4. O 1s + Pd 3$p_{3/2}$ spectra of graphite (a) subjected to ion etching, (*1*) HOPG-A, and (b) additional treatment in air at 300°C, (*1*) HOPG-A(O), and the samples of Pd deposited on (a) HOPG-A and (b) HOPG-A(O) (*2*) before and (*3*) after interaction with NO$_2$ under the conditions specified in Table 1.

time, a distribution between the states of oxygen changed in favor of compounds with ether and phenol groups, which correspond to a line with a binding energy of ~531 eV (Fig. 4b, spectrum *3*). The line belonging to palladium underwent a slight shift toward higher binding energies by ~0.2 eV, and its intensity slightly decreased (Fig. 4b, spectrum *3*).

Previously, we demonstrated the resistance of a carbon support in the Pd/C system to oxidants using the interaction of Pd/Sibunit samples with NO$_2$ as an example and hypothesized that it was caused by surface oxygen present in the composition of Sibunit [27]. In this study, as well as in previous works [28, 29], we found that the interaction of NO$_2$ with palladium supported by vacuum deposition on graphite, the surface of which did almost not contain oxygen, led to intense oxidation of the carbon material already at room temperature, and it was accompanied by destruction of 10−15 or more graphene layers and the formation of surface oxygen-containing carbon compounds. The

introduction of oxygen into the composition of HOPG by its preliminary treatment in air before the deposition of palladium led to the fact that graphite in the Pd/O-HOPG system became resistant to NO$_2$. In this case, the stability of graphite increased with the surface concentration of oxygen. Based on this observation, we hypothesized that, in both Sibunit and oxidized graphite, oxygen atoms on the surface of the carbon material block sites where oxidation could be initiated. The maximum atomic ratio [O]/[C] achieved in this work for HOPG-A after treatment in air was 0.024, which is significantly lower than that for Sibunit used previously [27]; the [O]/[C] ratios for this Sibunit in the initial state and after heating in a vacuum at 300 and 600°C were 0.100, 0.075, and 0.058, respectively. It should be noted that, in the sample prepared on HOPG subjected to ion etching (Pd/C-A), graphite showed a slightly lower tendency to oxidize than that in the sample on vacuum-annealed HOPG (Pd/C). This result seems unusual because HOPG-A, which

contains a significant concentration of surface defects, should be more easily oxidized to NO_2. Previously, we suggested that the observed difference in behavior may be associated with a higher palladium content of the Pd/C sample ($[Pd]/[C] = 0.0067$) than that of the Pd/C-A sample ($[Pd]/[C] = 0.0047$). However, in the light of the results obtained in this work, it should be concluded that the reason is, apparently, the presence of a certain amount of oxygen on the surface of HOPG-A ($[O]/[C] = 0.0035$), which is several times greater than that of HOPG ($[O]/[C] = 0.0004$).

CONCLUSIONS

The results presented show that the introduction of oxygen into the surface composition of HOPG at the stage of preparation of model samples with supported palladium radically changed their properties with respect to the subsequent interaction with nitrogen dioxide. Thus, the treatment of Pd/C and Pd/C-A samples, which were prepared with the use of HOPG with minimum surface oxygen content as a support, in NO_2 was accompanied by the intense oxidation of graphite and the incorporation of palladium particles into its surface layers. As a result, the XPS spectra showed a sharp decrease in the intensity of the photo and, to an even greater extent, Auger lines of palladium due to screening of the metal by the support material. Upon the interaction of Pd/C(O) and Pd/C-A(O) oxidized samples, which were prepared using HOPG with a relatively high oxygen concentration on the surface ($[O]/[C] \approx 0.01{-}0.02$), with NO_2, the carbon support remained almost unchanged, while palladium particles were oxidized to form the oxide PdO. In addition, the intensity ratios of the palladium and carbon lines changed insignificantly, and, consequently, the surface structure in these samples did not experience significant destruction.

ACKNOWLEDGMENTS

FUNDING

CONFLICT OF INTEREST

The authors declare that they have no conflicts of interest.

REFERENCES

1. Yoon, B. and Wai, C.M., *J. Am. Chem. Soc.,* 2005, vol. 127, p. 17174.

2. Mori, A., Miyakawa, Y., Ohashi, E., Haga, T., Maegawa, T., and Sajiki, H., *Org. Lett.,* 2006, vol. 8, p. 3279.

3. Deliy, I.V. and Simakova, I.L., *Russ. Chem. Bull. Int. Ed.,* 2008, vol. 57, p. 2056.

4. Deliy, I.V., Simakova, I.L., Ravasio, N., and Psaro, R., *Appl. Catal. A: Gen.,* 2009, vol. 357, p. 170.

5. Monguchi, Y., Mizuno, M., Ichikawa, T., Fujita, Y., Murakami, E., Hattori, T., Maegawa, T., Sawama, Y., and Sajiki, H., *J. Org. Chem.,* 2017, vol. 82, p. 10939.

6. Althikrallah, H., Kunstmann-Olsen, C., Kozhevnikova, E.F., and Kozhevnikov, I.V., *Catalysts,* 2020, vol. 10, p. 1171.

7. Ukisu, Y. and Miyadera, T., *React. Kinet. Catal. Lett.,* 2004, vol. 81, p. 305.

8. Chen, L., Yang, K., Liu, H., and Wang, X., *Carbon,* 2008, vol. 46, p. 2137.

9. Yuan, Z., Stephan, R., Hanf, M.C., Becht, J.M., Le Drian, C., Hugentobler, M., Harbich, W., and Wetzel, P., *Eur. Phys. J. D,* 2011, vol. 63, p. 401.

10. Song, S., Wang, Y., and Yan, N., *Molec. Catal.,* 2018, vol. 454, p. 87.

11. Li, F., Zhang, B., Wang, E., and Dong, S., *J. Electroanal. Chem.,* 1997, vol. 422, p. 27.

12. Gao, G.-Y., Guo, D.-J., and Li, H.-L., *J. Power Sources,* 2006, vol. 162, p. 1094.

13. Mazumder, V. and Sun, S., *J. Am. Chem. Soc.,* 2009, vol. 131, p. 4588.

14. Chen, L., Hu, G., Zou, G., Shao, S., and Wang, X., *Electrochem. Commun.,* 2009, vol. 11, p. 504.

15. Yermakov, Y.I., Surovikin, V.F., Plaksin, G.V., Semikolenov, V.A., Likholobov, V.A., Chuvilin, A.V., and Bogdanov, S.V., *React. Kinet. Catal. Lett.,* 1987, vol. 33, p. 435.

16. Simonov, P.A. and Likholobov, V.A., Physicochemical aspects of preparation of carbon-supported noble metal catalysts, in *Catalysis and Electrocatalysis at Nanoparticle Surfaces,* Wieckowski, A., Savinova, E.R., and Vayenas, C.G., Eds., Boca Raton, FL: CRC Press, 2003, ch. 12, p. 409.

17. Simakova, O.A., Simonov, P.A., Romanenko, A.V., and Simakova, I.L., *React. Kinet. Catal. Lett.,* 2008, vol. 95, p. 3.

18. Lokteva, E.S., Rostovshchikova, T.N., Kachevskii, S.A., Golubina, E.V., Smirnov, V.V., Stakheev, A.Yu., Telegina, N.S., Gurevich, S.A., Kozhevin, V.M., and Yavsin, D.A., *Kinet. Catal.,* 2008, vol. 49, p. 748.

19. Gudarzi, D., Simakova, O.A., Hernandez Carucci, J.R., Biasi, P.D., Eranen, K., Kolehmainen, E., Turunen, I., Murzin, D.Y., and Salmi, T., *Chem. Eng. Trans.,* 2010, vol. 21, p. 925.

20. Romanenko, A.V., Voropaev, I.N., Abdullina, R.M., and Chumachenko, V.A., *Solid Fuel Chem.,* 2014, vol. 48, p. 356.

21. Simonov, P.A., Romanenko, A.V., and Likholobov, V.A., *Solid Fuel Chem.,* 2014, vol. 48, p. 364.

22. Belskaya, O.B., Mironenko, R.M., Gulyaeva, T.I., Trenikhin, M.V., and Likholobov, V.A., *Russ. Chem. Bull. Int. Ed.,* 2018, vol. 67, p. 71.

23. Lokteva, E.S. and Golubina, E.V., *Pure Appl. Chem.,* 2019, vol. 91, p. 609.

24. Golub, F.S., Beloshapkin, S., Gusel'nikov, A.V., Bolotov, V.A., Parmon, V.N., and Bulushev, D.A., *Energies,* 2019, vol. 12, p. 3885.

25. Shlyapin, D.A., Glyzdova, D.V., Afonasenko, T.N., Temerev, V.L., and Tsyrul'nikov, P.G., *Kinet. Catal.,* 2019, vol. 60, p. 446.

26. German, D., Pakrieva, E., Kolobova, E., Carabineiro, S.A.C., Stucchi, M., Villa, A., Prati, L., Bogdanchikova, N., Corberan, V.C., and Pestryakov, A., *Catalysts,* 2021, vol. 11, p. 115.

27. Smirnov, M.Yu., Kalinkin, A.V., Simonov, P.A., and Bukhtiyarov, V.I., *Kinet. Catal.,* 2022, vol. 63, p. 532.

28. Smirnov, M.Yu., Kalinkin, A.V., Sorokin, A.M., and Bukhtiyarov, V.I., *Kinet. Catal.,* 2020, vol. 61, p. 637.

29. Smirnov, M.Yu., Kalinkin, A.V., Sorokin, A.M., and Bukhtiyarov, V.I., *Kinet. Catal.,* 2020, vol. 61, p. 907.

30. Moulder, J.F., Stickle, W.F., Sobol, P.E., and Bomben, K.D., *Handbook of X-ray Photoelectron Spectroscopy,* Eden Prairie: Perkin-Elmer Co, 1992.

31. Kalinkin, A.V., Sorokin, A.M., Smirnov, M.Yu., and Bukhtiyarov, V.I., *Kinet. Catal.,* 2014, vol. 55, p. 354.

32. Schnyder, B., Alliata, D., Kotz, R., and Siegenthaler, H., *Appl. Surf. Sci.,* 2001, vol. 173, p. 221.

33. Yang, D.-Q. and Sacher, E., Surf. Sci., 2002, vol. 504, p. 125.

34. Rousseau, B., Estrade-Szwarckopf, H., Thomann, A.-L., and Brault, P., *Appl. Phys. A,* 2003, vol. 77, p. 591.

35. Blume, R., Rosenthal, D., Tessonnier, J.-P., Li, H., Knop-Gericke, A., and Schlogl, R., *ChemCatChem,* 2015, vol. 7, p. 2871.

36. Susi, T., Pichler, T., and Ayala, P., *Beilstein J. Nanotechnol.,* 2015, vol. 6, p. 177.

37. Paredes, J.I., Martínez-Alonso, A., and Tascon, J.M.D., *Langmuir,* 2007, vol. 23, p. 8932.

38. Favaro, M., Agnoli, S., Perini, L., Durante, C., Gennaro, A., and Granozzi, G., *Phys. Chem. Chem. Phys.,* 2013, vol. 15, p. 2923.

39. Merel, P., Tabbal, M., Chaker, M., Moisa, S., and Margot, J., *Appl. Surf. Sci.,* 1998, vol. 136, p. 105.

40. Utsumi, S., Honda, H., Hattori, Y., Kanoh, H., Takahashi, K., Sakai, H., Abe, M., Yudasaka, M., Iijima, S., and Kaneko, K., *J. Phys. Chem. C,* 2007, vol. 111, p. 5572.

41. Stobinski, L., Lesiak, B., Malolepszy, A., Mazurkiewicz, M., Mierzwa, B., Zemek, J., Jiricek, P., and Bieloshapka, I., *J. Electron Spectrosc. Relat. Phenom.,* 2014, vol. 195, p. 145.

42. Kovtun, A., Jones, D., Dell'Elce, S., Treossi, E., Liscio, A., and Palermo, V., *Carbon,* 2019, vol. 143, p. 268.

43. Stanczyk, K., Dziembaj, R., Piwowarsca, Z., and Witkowski, S., *Carbon,* 1995, vol. 33, p. 1383.

44. Kostecki, R., Schnyder, B., Alliata, D., Song, X., Kinoshita, K., and Kotz, R., *Thin Solid Films,* 2001, vol. 396, p. 36.

45. Martínez, M.T., Callejas, M.A., Benito, A.M., Cochet, M., Seeger, T., Anson, A., Schreiber, J., Gordon, C., Marhic, C., Chauvet, O., Fierro, J.L.G., and Maser, W.K., *Carbon,* 2003, vol. 41, p. 2247.

46. Hou, S., Su, S., Kasner, M.L., Shah, P., Patel, K., and Madarang, C.J., *Chem. Phys. Lett.,* 2010, vol. 501, p. 68.

47. Ghosh, B., Sarma, S., Pontsho, M., and Ray, S.C., *Diamond Relat. Mater.,* 2018, vol. 89, p. 35.

48. Yang, D., Velamakanni, A., Bozoklu, G., Park, S., Stoller, M., Piner, R.D., Stankovich, S., Jung, I., Field, D.A., Ventrice, C.A., and Ruoff, R.S., *Carbon,* 2009, vol. 47, p. 145.

49. Figueiredo, J.L. and Pereira, M.F.R., *Catal. Today,* 2010, vol. 150, p. 2.

50. Ganguly, A., Sharma, S., Papakonstantinou, P., and Hamilton, J., *J. Phys. Chem. C,* vol. 115, p. 17009.

51. Ansón-Casaos, A., Puértolas, J.A., Pascual, F.J., Hernández-Ferrer, J., Castell, P., Benito, A.M., Maser, W.K., and Martínez, M.T., *Appl. Surf. Sci.,* 2014, vol. 301, p. 264.

52. Nosova, L.V., Stenin, M.V., Nogin, Yu.N., and Ryndin, Yu.A., *Appl. Surf. Sci.,* 1992, vol. 55, p. 43.

53. Aiyer, H.N., Vijayakrishnan, V., Subbanna, G.N., and Rao, C.N.R., *Surf. Sci.,* 1994, vol. 313, p. 392.

54. Glyzdova, D.V., Afonasenko, T.N., Khramov, E.V., Leont'eva, N.N., Prosvirin, I.P., Bukhtiyarov, A.V., and Shlyapin, D.A., *Appl. Catal. A: Gen.,* 2020, vol. 600, p. 117627.

55. Smirnov, M.Yu., Klembovskii, I.O., Kalinkin, A.V., and Bukhtiyarov, V.I., *Kinet. Catal.,* 2018, vol. 59, p. 786.

56. Zemlyanov, D., Azalos-Kiss, B., Kleimenov, E., Teschner, D., Zafeiratos, S., Havecker, M., Knop-Gericke, A., Schlogl, R., Gabasch, H., Unterberger, W., Hayek, K., and Klotzer, B., *Surf. Sci.,* 2006, vol. 600, p. 983.

57. Kibis, L.S., Titkov, A.I., Stadnichenko, A.I., Koscheev, S.V., and Boronin, A.I., *Appl. Surf. Sci.,* 2009, vol. 255, p. 9248.

58. Peuckert, M., *J. Phys. Chem.,* 1985, vol. 89, p. 2481.

59. Fleisch, T.H. and Mains, G.J., *J. Phys. Chem.,* 1986, vol. 90, p. 5317.

60. Pillo, T., Zimmermann, R., Steiner, P., and Hufner, S., *J. Phys.: Condens. Matter,* 1997, vol. 9, p. 3987.

61. Militello, M.C. and Simko, S.J., *Surf. Sci. Spectra,* 1997, vol. 3, p. 395.

62. Brun, M., Berthet, A., and Bertolini, J.C., *J. Electron Spectrosc. Relat. Phenom.,* 1999, vol. 104, p. 55.

63. Mirkelamoglu, B. and Karakas, G., *Appl. Catal. A: Gen.,* 2006, vol. 299, p. 84.

64. Titkov, A.I., Salanov, A.N., Koscheev, S.V., and Boronin, A.I., *Surf. Sci.,* 2006, vol. 600, p. 4119.

65. Wang, J., Yun, Y., and Altman, E.I., *Surf. Sci.,* 2007, vol. 601, p. 3497.

Translated by V. Makhlyarchuk